

Path integral treatment of coherence effects in charmonium production in nuclear ultra-peripheral collisions

J. Óbertová^{a,*} and J. Nemchik^{a,b}

^a*Faculty of Nuclear Sciences and Physical Engineering, Czech Technical University in Prague, Břehová 7, 115 19, Prague, Czech Republic*

^b*Institute of Experimental Physics SAS, Watsonova 47, 04001 Košice, Slovakia*

E-mail: jaroslava.obertova@fjfi.cvut.cz, jan.nemcik@fjfi.cvut.cz

We present for the first time a revised study of charmonium production in nuclear ultra-peripheral collisions (UPC) based on a rigorous Green function formalism. This formalism allows for the proper incorporation of the effects of color transparency, as well as the quantum coherence inherent in the higher twist quark shadowing related to the $Q\bar{Q}$ Fock component of the photon. The significance of this effect gradually decreases towards forward and/or backward rapidities. In the LHC kinematic region we additionally incorporate within the same formalism the leading twist gluon shadowing corrections related to higher multi-gluon photon fluctuations. They represent a dominant source of nuclear phenomena in the mid-rapidity region. Model predictions for the rapidity distributions $d\sigma/dy$ are in good agreement with available UPC data on coherent charmonium production at RHIC and the LHC. They can also be verified by future measurements at the LHC, as well as at EIC.

*42nd International Conference on High Energy Physics (ICHEP24),
18-24 July 2024
Prague, Czech Republic*

*Speaker

1. Introduction

The study of heavy quarkonium production in heavy-ion collisions can help us to extend our understanding of the QCD dynamics, as well as manifestations of various nuclear effects, such as quantum coherence, color transparency, gluon shadowing and gluon saturation. The production of charmonia in photo-nuclear reactions ($Q^2 \approx 0$) is recently intensively studied in ultra-peripheral Pb-Pb collisions at the Large Hadron Collider (LHC) and in Au-Au UPC at Relativistic Heavy Ion collider (RHIC). Here, the gluon shadowing (GS) corrections at LHC energies and the reduced effects of quantum coherence in the forward/backward rapidity region are often neglected or incorporated inaccurately in most of the current calculations. In this contribution, we refer on our study of coherent (elastic) photoproduction of charmonia, $\gamma A \rightarrow VA$ [$V = J/\psi(1S), \psi'(2S)$], in UPC, extended to charmonium electroproduction, $\gamma^* A \rightarrow VA$, in expected Electron-Ion-Collider (EIC) kinematic region within the light-front (LF) color dipole approach. We focus on the proper treatment of reduced effects of the coherence length using the Green function technique.

2. Green function formalism for the coherent photo-nuclear reaction

The cross section for photo-nuclear reaction in a heavy-ion UPC, derived in the one-photon-exchange approximation and expressed in the rest frame of the target nucleus A [1], is defined as follows:

$$k \frac{d\sigma}{dk} = \int d^2\tau \int d^2b n(k, \vec{b} - \vec{\tau}, y) \frac{d^2\sigma_A(s, b)}{d^2b} + \{y \rightarrow -y\}. \quad (1)$$

Here the rapidity variable $y = \ln[s/(M_V\sqrt{s_N})] \approx \ln[(2kM_N + M_N^2)/(M_V\sqrt{s_N})]$ with M_N and M_V being the nucleon and vector meson mass, respectively, $\sqrt{s_N}$ is the collision energy and k is the photon energy related to the square of the photon-nucleon center-of-mass (c.m.) energy $W^2 = 2M_N k + M_N^2 - Q^2 \approx s - Q^2$, where s is the photon-nucleon c.m. energy squared. The variable $\vec{\tau}$ is the relative impact parameter of a nuclear collision and \vec{b} is the impact parameter of the photon-nucleon collision relative to the center of one of the nuclei. It holds that $\tau > 2R_A$, for a UPC of identical nuclei with the nuclear radius R_A . The variable $n(k, \vec{b})$ represents the photon flux induced by a projectile nucleus. The corresponding formula for the coherent production cross section has the following form [2, 3]

$$\frac{d^2\sigma_A^{coh}(s, b)}{d^2b} = \frac{1}{4} \left| \int_{-\infty}^{\infty} dz \rho_A(b, z) H_1(s, b, z) \right|^2, \quad (2)$$

where $\rho_A(b, z)$ is the nuclear density distribution employed in the realistic Wood-Saxon form. The function $H_1(s, b, z)$ can be expressed within a rigorous path integral technique as

$$H_1(s, b, z) = \int_0^1 d\alpha \int d^2r_1 d^2r_2 \Psi_V^*(\vec{r}_2, \alpha) G_{Q\bar{Q}}(z' \rightarrow \infty, \vec{r}_2; z, \vec{r}_1) \sigma_{Q\bar{Q}}(r_1, s) \Psi_{\gamma(\gamma^*)}(\vec{r}_1, \alpha). \quad (3)$$

Here, $\Psi_V(\vec{r}, \alpha)$ is the LF wave function for heavy quarkonium, obtained by the Terent'ev boosting prescription [4] and including the correction due to the Melosh spin rotation effect [5], and $\Psi_{\gamma(\gamma^*)}(\vec{r}, \alpha)$ is the LF distribution of the $Q\bar{Q}$ Fock component of the quasi-real (transversely polarized) or virtual photon. Variable \vec{r} is the transverse separation of the $Q\bar{Q}$ fluctuation (dipole) and

$\alpha = p_Q^+ / p_\gamma^+$ is the boost-invariant fraction of the photon momentum carried by a heavy quark (or antiquark). The dipole cross section $\sigma_{Q\bar{Q}}(r, s)$ in Eq. (3) describes the interaction of the $Q\bar{Q}$ dipole with the nucleon target. The Green function $G_{Q\bar{Q}}(z' \rightarrow \infty, \vec{r}_2; z, \vec{r}_1)$, which describes the evolution of a $Q\bar{Q}$ pair between points \vec{r}_1, z and \vec{r}_2, z' , satisfies the two-dimensional Schrödinger equation [6]

$$i \frac{d}{dz_2} G_{Q\bar{Q}}(z_2, \vec{r}_2; z_1, \vec{r}_1) = \left[\frac{\eta^2 - \Delta_{r_2}}{2k\alpha(1-\alpha)} + V_{Q\bar{Q}}(z_2, \vec{r}_2, \alpha) \right] G_{Q\bar{Q}}(z_2, \vec{r}_2; z_1, \vec{r}_1), \quad (4)$$

where $\eta^2 = m_Q^2 + \alpha(1-\alpha)Q^2$, m_Q is the heavy quark mass and Laplacian Δ_{r_2} acts on the coordinate r_2 . Important ingredient of the Schrödinger equation is the complex $Q\bar{Q}$ potential in the LF frame, $V_{Q\bar{Q}}(z_2, \vec{r}_2, \alpha)$. The imaginary part of the LF potential controls the attenuation of the $Q\bar{Q}$ pair in the medium and the corresponding real part describes the interaction between the Q and \bar{Q} . The values of the real part of the LF potential for arbitrary model of $Q - \bar{Q}$ interaction are obtained numerically, as described in Ref. [3], by solving the LF Schrödinger equation for $\Psi_V(\vec{r}_2, \alpha)$.

The kinetic term in Eq. (4) includes the coherence length (CL), $l_c = 1/q_L$, with q_L being the longitudinal momentum transfer defined as

$$q_L(z) = \frac{M_{Q\bar{Q}}^2(z) + Q^2}{2k} \Rightarrow \frac{\eta^2 - \Delta_{r_2}}{2k\alpha(1-\alpha)}, \quad (5)$$

where $M_{Q\bar{Q}}^2 = (m_Q^2 + q_T^2)/\alpha(1-\alpha)$ is the $Q\bar{Q}$ effective mass and $q_T^2 \Rightarrow -\Delta_r$ is the quark transverse momentum. The condition $l_c \geq R_A$ controls the onset of the quantum coherence effect related to $Q\bar{Q}$ Fock component of the photon and leading to higher twist quark shadowing. Another effect, known as the color transparency (CT), is responsible for the final state absorption of produced quarkonium [2, 3]. The onset of CT is controlled by the transverse size evolution of a $Q\bar{Q}$ pair propagating through the medium and is also incorporated in the Green function formalism.

In the electroproduction of heavy quarkonia at EIC energies, we evaluate the total cross section for quarkonium production on nuclear target as follows,

$$\sigma_{\gamma^* A \rightarrow J/\psi A}(s, b) = \int d^2b \frac{d^2\sigma_A^{coh}(s, b)}{d^2b}. \quad (6)$$

Then, we express the nucleus-to-nucleon ratio (*nuclear transparency*) as

$$R_A^{coh}(J/\psi) = \frac{\sigma_{\gamma^* A \rightarrow J/\psi A}}{A \sigma_{\gamma^* N \rightarrow J/\psi N}} \quad (7)$$

where $\sigma_{\gamma^* N \rightarrow J/\psi N}$ is the total cross section for J/ψ production on a nucleon target. More details about the formalism can be found in Ref. [3].

We also include in Eq. (3) a small correction due to the real part of the $\gamma^* N \rightarrow J/\psi N$ amplitude by performing the following replacement [7–9],

$$\sigma_{Q\bar{Q}}(r, s) \Rightarrow \sigma_{Q\bar{Q}}(r, s) \left(1 - i \frac{\pi}{2} \Lambda \right), \quad \Lambda = \frac{\partial \ln \sigma_{Q\bar{Q}}(r, s)}{\partial \ln s}. \quad (8)$$

Another phenomenon that affects heavy quarkonium production in photo-nuclear reactions in UPC is gluon shadowing. The effect of GS has to be additionally included as a shadowing correction

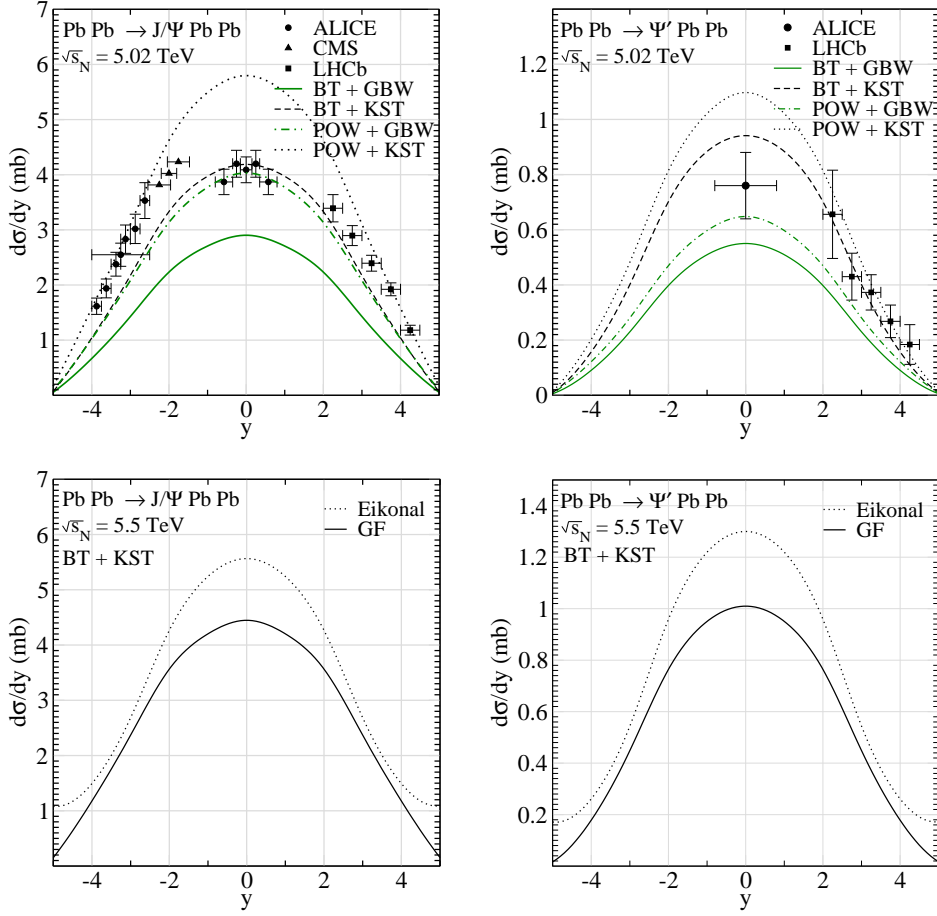


Figure 1: Rapidity distributions of coherent cross section for photoproduction of J/ψ (left) and ψ' (right) in UPC at LHC energies $\sqrt{s_N} = 5.02$ TeV (top panel) and 5.5 TeV (bottom panel). The data for $d\sigma/dy$ from ALICE [10], LHCb [11, 12] and CMS [13] Collaborations are shown for comparison. Figure is adopted from Ref. [3].

corresponding to higher Fock components of the photon containing gluons. It was incorporated as a reduction of $\sigma_{Q\bar{Q}}(r, s)$ in nuclear reactions with respect to processes on the nucleon [14],

$$\sigma_{Q\bar{Q}}(r, x) \Rightarrow \sigma_{Q\bar{Q}}(r, x) \cdot R_G(x, b). \quad (9)$$

The correction factor $R_G(x, b)$ was calculated within the Green function formalism as a function of the nuclear impact parameter b and the Bjorken variable x .

3. Results

We calculated the coherent charmonium photoproduction in UPC at LHC energies according to Eq. (1), as well as the electroproduction at EIC energies using Eqs. (6) and (7). In Figure 1, top panels, we present comparison of our model predictions for the rapidity distributions $d\sigma/dy$ of coherent $J/\psi(1S)$ (left panel) and $\psi'(2S)$ (right panel) photoproduction in UPC at c.m. collision energy $\sqrt{s_N} = 5.02$ TeV with available data. Our results were obtained for charmonium wave

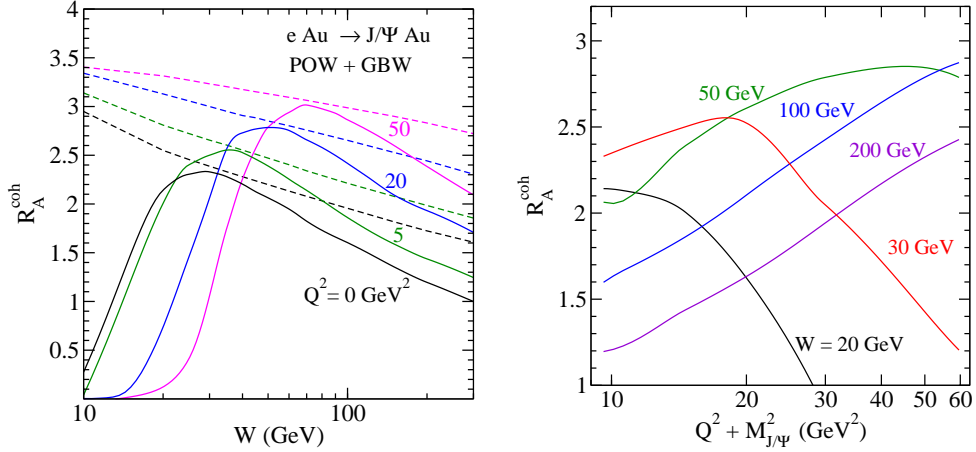


Figure 2: Ratio R_A^{coh} for J/ψ coherent production on the gold target as a function of c.m. energy W at several fixed values of photon virtuality $Q^2 = 0, 5, 20$ and 50 GeV^2 (left panel). Right panel shows the ratio R_A^{coh} as a function of $Q^2 + M_{J/\psi}^2$ at several fixed values of $W = 20, 30, 50, 100$ and 200 GeV . Figure is adopted from Ref. [3].

functions generated by two $c\bar{c}$ potential models, POW [15, 16] (dotted and dot-dashed lines) and BT [17] (solid and dashed lines). For the dipole cross sections $\sigma_{Q\bar{Q}}$ we employed the GBW [18] (solid and dot-dashed lines) and KST [2] (dashed and dotted lines) parametrizations. Our predictions based on the Green function formalism manifest a rather good agreement with data. Bottom panels of Figure 1 show the prediction for rapidity distributions of coherent charmonium cross section at larger $\sqrt{s_N} = 5.5 \text{ TeV}$, which is planned to be measured at the LHC. Here, solid lines represent calculations within a rigorous path integral technique. The dotted lines are based on the Eikonal approximation ($l_c \gg R_A$ in Eq. (3)) for production cross section and without GS corrections. The difference between solid and dotted lines at midrapidities illustrates the net GS effect. At forward/backward rapidities, the GS vanishes and the difference between the two lines is caused by the reduced effects of quantum coherence when $l_c \lesssim R_A$.

In Figure 2, we present the ratio R_A^{coh} from Eq. (7) as a function of the c.m. energy W (left panel) and as a function of $Q^2 + M_{J/\psi}^2$ (right panel) for electroproduction of $J/\psi(1S)$ on a gold target. The values of R_A^{coh} were obtained using the charmonium LF wave function generated by the POW $c\bar{c}$ interaction potential and the GBW model for $\sigma_{Q\bar{Q}}$ fitted to data for photon virtualities $Q^2 \leq 50 \text{ GeV}^2$ [18]. In the left panel of Figure 2, our results show significant leading twist corrections, rising with the photon energy, as differences between solid (the Green function formalism with GS) and dashed (Eikonal approximation without GS) lines at large W . At small photon energies, up to the position of maximal R_A^{coh} values, the difference is caused by the effect of reduced coherence length, as $l_c \lesssim R_A$. Right panel of Figure 2 represents the $Q^2 + M_{J/\psi}^2$ -behavior of R_A^{coh} at different values of photon energy W . At large $W = 100$ and 200 GeV , CL is long enough, $l_c > R_A$, to neglect its variation with Q^2 and the rise of R_A^{coh} with Q^2 is a net manifestation of CT. The effect of reduced CL is visible at lower energies, $W < 50 \text{ GeV}$, as decrease of R_A^{coh} with Q^2 .

Our predictions for the onset of reduced coherence effects and gluon shadowing can be tested by future experiments at EIC. The proper treatment of the shadowing and absorption effects in the

nuclear medium within a rigorous path integral technique may be crucial for the future conclusive evidence of expected gluon saturation effects at large energies.

Acknowledgments

The work of J.N. was partially supported by the Slovak Funding Agency, Grant No. 2/0020/22. Computational resources were provided by the e-INFRA CZ project (ID:90254), supported by the Ministry of Education, Youth and Sports of the Czech Republic.

References

- [1] C. A. Bertulani, S. R. Klein and J. Nystrand, *Ann. Rev. Nucl. Part. Sci.* **55** (2005) 271.
- [2] B. Kopeliovich, J. Nemchik, A. Schafer and A. Tarasov, *Phys. Rev. C* **65** (2002) 035201.
- [3] J. Nemchik and J. Obertova, *Phys. Rev. D* **110** (2024) 054015.
- [4] M.V. Terentev, *Sov. J. Nucl. Phys.* **24** (1976) 106. [*Yad. Fiz.* **24** (1976) 207].
- [5] H.J. Melosh, *Phys. Rev. D* **9** (1974) 1095.
- [6] B.Z. Kopeliovich, A. Schafer and A.V. Tarasov, *Phys. Rev. D* **62** (2000) 054022.
- [7] J. B. Bronzan, G. L. Kane and U. P. Sukhatme, *Phys. Lett. B* **49** (1974) 272.
- [8] J. Nemchik, N. N. Nikolaev, E. Predazzi and B. Zakharov, *Z. Phys. C* **75** (1997) 71.
- [9] J. R. Forshaw, R. Sandapen and G. Shaw, *Phys. Rev. D* **69** (2004) 094013.
- [10] S. Acharya *et al.* [ALICE], *Phys. Lett. B* **798** (2019) 134926; *Eur. Phys. J. C* **81** (2021) 712.
- [11] A. Bursche [LHCb], *Nucl. Phys. A* **982** (2019) 247.
- [12] R. Aaij *et al.* [LHCb], *JHEP* **06** (2023) 146.
- [13] A. Tumasyan *et al.* [CMS], *Phys. Rev. Lett.* **131** (2023) 262301.
- [14] B. Kopeliovich, A. Tarasov and J. Hufner, *Nucl. Phys. A* **696** (2001) 669.
- [15] A. Martin, *Phys. Lett. B* **93** (1980) 338.
- [16] N. Barik and S.N. Jena, *Phys. Lett. B* **97** (1980) 265.
- [17] W. Buchmuller and S.H.H. Tye, *Phys. Rev. D* **24** (1981) 132.
- [18] K. Golec-Biernat and S. Sapeta, *JHEP* **03** (2018) 102.